PERGAMON

International Journal of Impact Engineering 26 (2001) 613–624

INTERNATIONAL JOURNAL OF IMPACT ENGINEERING

www.elsevier.com/locate/ijimpeng

DEBRIS CLOUDS PRODUCED BY THE HYPERVELOCITY IMPACT OF NONSPHERICAL PROJECTILES

ANDREW J. PIEKUTOWSKI

University of Dayton Research Institute, 300 College Park Avenue, Dayton, Ohio 45469-0182

Abstract—The significant features of debris clouds produced by the normal impact of spheres are described and compared with the features of debris clouds produced by the normal impact of nonspherical projectiles. Projectile shape and orientation at impact are shown to have a significant effect on the ability of a single-sheet bumper shield to promote the breakup of the projectile and the dispersion of the projectile fragments. The debris clouds produced by the normal impact of spheres are "relatively benign" in terms of their potential for damage to the rear wall of a spacecraft. Debris clouds produced by nonspherical projectiles contain one or more very large fragments at their leading edge that significantly threaten rear wall integrity.

Keywords: aluminum projectiles, aluminum spheres, bumper shields, damaged spheres, disks, inclined cylinders, irregular-shaped projectiles, nonspherical projectiles, projectile shape effects, projectile inclination, rear wall damage, short rods, witness plate damage, zinc projectiles.

INTRODUCTION

Although aluminum spheres are commonly accepted as a standard projectile for use in evaluating the impact resistance of spacecraft components and shields, it is very unlikely that micrometeoroids and fragments of orbital debris will be spherical. Morrison [1] had recognized the effect of projectile shape on the impact resistance of double-walled structures and had shown that cylinders impacting in the direction of their axis were considerably more effective penetrators than spheres of the same mass. In another study, the inclination of right-cylinder aluminum projectiles at impact was shown to affect the level of damage inflicted on the rear wall of a double-sheet structure [2]. Cylinders that impacted with their axis aligned coincident with the shot-line axis produced the least damage to a rear wall while cylinders inclined at approximately 45 degrees produced significantly more damage. Projectile shape and orientation at impact are critical parameters to be considered when assessing the lethality of nonspherical projectiles.

EXPERIMENTAL PROCEDURES

All of the tests described in this paper were performed in the University of Dayton Research Institute Impact Physics Laboratory. Impact velocity determinations were made with use of four laser-photodetector systems installed at various locations along the flight path of the projectile. Accuracy of the impact velocity determination was better than ± 0.5 percent. The tests were performed using 2017-T4 aluminum spheres with several diameters and a variety of nonspherical aluminum and zinc projectiles. Various thicknesses of 6061-T6 aluminum and zinc sheets were used as bumpers. Four pairs of fine-source, soft, flash x-rays were used to observe the projectile and the debris cloud. The x-ray heads were accurately positioned on the target chamber to

0734-743X/01/$ - see front matter
PII: S0734-743X(01)00122-1

provide simultaneous orthogonal views of the debris clouds. The first pair of x-ray heads was used to view and record the position of the projectile a few microseconds before impact to verify projectile integrity and to permit an accurate determination of the time after impact for the three views taken of the debris cloud after its formation.

SPHERICAL PROJECTILES

Two views of a debris cloud are presented at the top of Fig. 1 to illustrate the three major features of a debris cloud produced by the impact of an aluminum sphere with a thin aluminum sheet. First, an ejecta veil, consisting almost entirely of bumper fragments, was ejected from the impact or front side of the bumper. Second, an expanding bubble of bumper debris was formed on the rear side of the bumper. Finally, there was a significant structure composed of projectile debris located inside and at the front of the external bubble of bumper debris.

An enlarged, late-time view of the internal structure of a debris cloud is presented at the bottom of Fig. 1. This internal structure was composed of a front, center, and rear element. For a 6.70 km/s impact shown at the top of Fig. 1, the front element consisted of finely divided, molten droplets of bumper and projectile. The disk-like center element was composed of a large number of solid slivers, comma-shaped, and/or chunky pieces of fragmented projectile and a single large chunky fragment of projectile that was located at the center of the disk and on the debris-cloud centerline. This central fragment was observed in all debris clouds where the bumper-sheet-thickness-to-projectile-diameter ratio, t/D, was less than 0.2. This central fragment represented the most severe threat to rear wall integrity [3]. The bulk of the post-impact projectile mass appeared to be concentrated in the center element. The rear element of the internal structure was a hemispherical shell of fragments spalled from the rear surface of the sphere. The internal structure of the debris cloud shown in Fig. 1 was the most significant feature of the debris cloud in terms of potential for rear-wall damage. In this paper, the term "debris cloud" is used synonymously with "internal structure."

The effects of a change in the t/D ratio and/or a change in impact velocity on the morphology of a debris-cloud produced by the normal impact of a sphere with a thin sheet are presented and discussed in detail in Ref. [4]. As the t/D ratio was increased and the impact velocity was held constant, a series of changes in the morphology of the internal-structure was observed. The diameter of the disk-like center element increased as the t/D ratio increased from 0.026 to 0.062 (shown in upper part of Fig. 1). At a t/D ratio of 0.084, the outer edges of the disk began to "bend over" and the disk formed a flat-bottomed bowl at t/D ratios of 0.163 and greater. The radial expansion of the hemispherical shell of spall fragments also increased as the t/D ratio increased. The size of the fragments in the center and rear elements decreased as the t/D ratio increased. In contrast to the growth of the center and rear element, the front element of the debris cloud did not experience a significant change in size, shape (a truncated cone), or radiographic density until the t/D ratio was greater than 0.102. At t/D ratios of 0.163 and greater, the front element was a spherical sector; it was not evident when the t/D ratio was 0.424. As the t/D ratio increased, a significantly larger fraction of the bumper became involved in the formation of the external bubble of debris.

In the following discussion of the effects of a change in the impact velocity on the debris cloud morphology, the t/D ratio will be held constant. When the impact velocity was below the spall-failure-threshold velocity, see Ref. [4], the sphere simply produced a hole in the aluminum sheet and continued to travel downrange intact. When the impact velocity was at or slightly above the spall-failure-threshold velocity, a spall failure developed inside the rear surface of the sphere, increased its radius and formed a shell that remained attached to the sphere. A slight flattening of the front of the sphere and the formation of a small piece of bumper that moved downrange slightly faster than the flattened sphere was also observed. As the impact velocity was increased, fragmentation of the sphere and an increase in the axial and diametral expansion

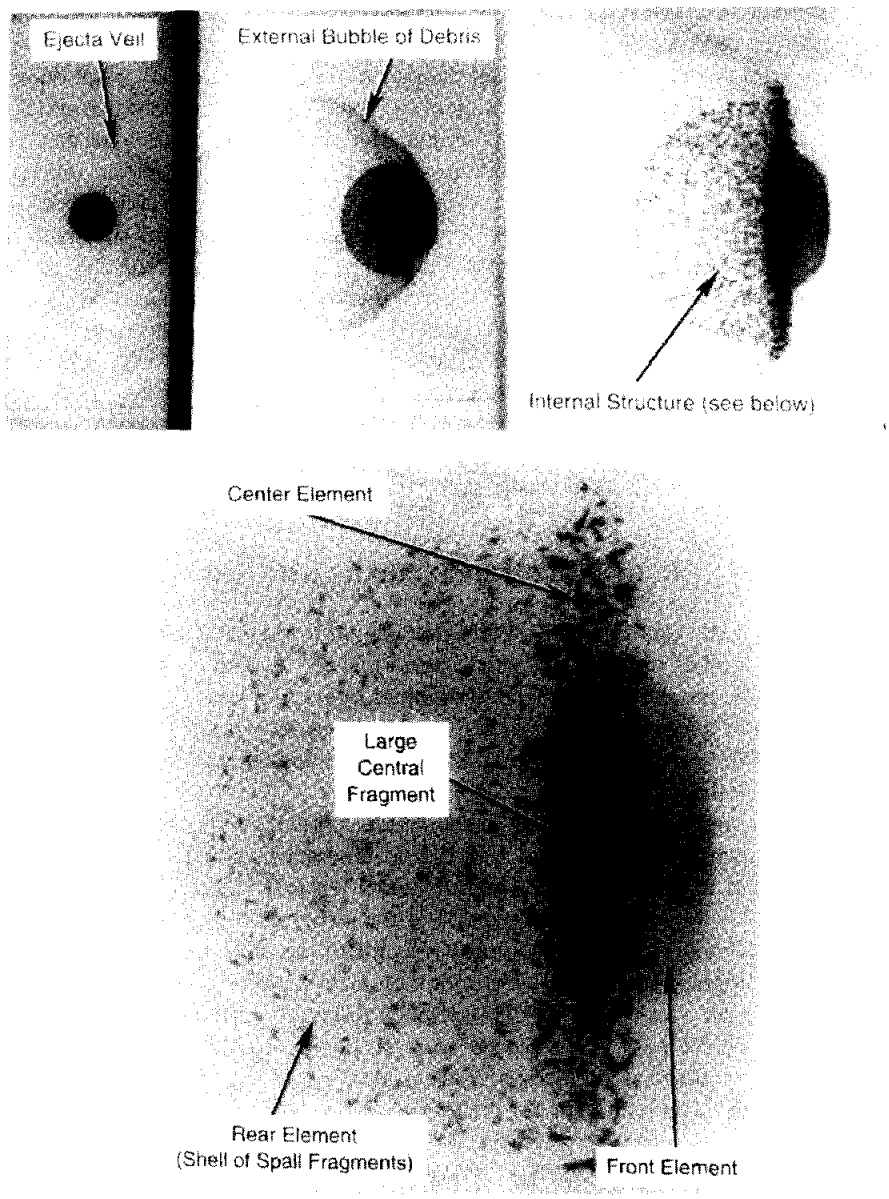

Fig. 1. Structural features of well-developed debris clouds formed by the normal impact of aluminum spheres with thin aluminum sheets.

of the internal structure was observed. The size of the fragments in the center element and the spall shell decreased quickly as the debris cloud transitioned from a deformed sphere to a well-developed debris cloud (i.e., contained all three elements of the internal structure).

The effects of a change in scale on debris cloud properties are described for a series of tests in Ref. [5]. In these tests, the projectile diameter was varied from 6.35 mm to 15.88 mm, a factor of 2.5, and the t/D ratio and impact velocity were held constant at 0.049 and 6.25 km/s, respectively. The shape and position of the major structural elements of the debris clouds produced by these four tests were qualitatively the same. The dimensions of the elements in the debris clouds differed only by the differences in the diameters of the spheres that produced them. An analysis of the size of the fragments in the debris clouds showed that the equivalent diameter of the large central fragment in the center element scaled with projectile diameter. The large central fragment

appeared to originate from near the center of the sphere and was a part of the sphere that remained intact after all processes that worked to reduce the size of the sphere were complete. The dimensions of fragments forming the shell of spall fragments at the rear of the debris cloud did not scale with projectile diameter. Formation of the spall-shell fragments was a shock-related process that was sensitive to rate effects and other material properties that did not scale.

The failure and fragmentation of an aluminum sphere that was initiated by an impact with a thin aluminum sheet was an orderly process. For impacts at the velocities and t/D ratios where the debris clouds were well developed, the front element was composed of finely divided fragments and/or molten droplets of bumper and projectile. The bulk of the post-impact projectile mass appeared to be concentrated in the disk-like center element and was composed of smaller pieces of fragmented projectile and a single large chunky projectile fragment that was located on the debris-cloud axis. The rear element of the internal structure was a hemispherical shell of fragments that spalled from the rear surface of the sphere. The material in these three elements would impact a rear wall during a finite time period. The most severe threat to rear wall integrity, the large central fragment, is located *behind* the front element and would strike material that was already damaged and weakened by the impact of the front element.

REGULAR-SHAPED PROJECTILES

Right circular cylinders and cylinders with other length-to-diameter ratios, L/D, have been used as projectiles in studies of spacecraft shield performance. As shown in [1], disks with L/D ratios of less than 1 are more effective penetrators than right cylinders with the same diameter. In [2], the orientation of a right circular cylinder at impact was shown to significantly change the shape of the debris cloud produced by the impact of the inclined cylinder and to affect the level of damage sustained by the rear wall.

The effects of a change in the L/D ratio of cylindrical projectiles on the shape of the debris cloud are shown in the radiographs presented in Fig. 2. The debris clouds shown in Fig. 2 were produced by the impact of a zinc sphere, a right cylinder, an $L/D = 3$ rod, and an $L/D = 0.058$ disk with zinc sheets. A more detailed description of the results of this series of tests performed for Sandia National Laboratory is provided in [6]. Details of the projectile used for each test are provided with the radiographs in Fig. 2. The morphological features of the debris clouds were unique for each projectile shape and the debris clouds produced different levels of damage to 2.44-mm-thick, 6061-T6 witness plates placed 15.2 cm downrange of the zinc bumpers. The features of the debris cloud for the zinc sphere were identical to the features of the $t/D = 0.16$ aluminum debris clouds. The rear walls for the test using the sphere was not perforated; the rear walls for the other three tests were perforated.

The right cylinder was inclined ~20 degrees when it struck the bumper sheet. Consequently, the debris cloud was distorted and asymmetric. Two features observed in the debris cloud for the test with the right-cylinder zinc projectiles were also observed in the debris clouds for the tests with right-cylinder aluminum projectiles [2], namely, an inclined, conical front-element with the point towards the front of the structure and a longer, denser, conical rear-element with the point at the rear of the element. The witness plate for this test had a 5.6-cm-long tear that was promoted by a line of craters and holes formed by fragments that were located in the region of the debris cloud where the front and rear elements joined.

The $L/D = 3$ rod impacted the bumper with its axis nearly coincident with the shot-line axis. As shown in the radiograph of the debris cloud, a conical front-element of bumper debris was formed. Eroded-projectile fragments formed a large, saucer-shaped structure around the conical front-element and at the front of the external bubble of debris. Approximately one-half of the rod remained intact and traveled at the original impact velocity after passing through the bumper sheet. The rear end of the rod simply passed through a 3.6-cm-diameter hole that was formed in the rear wall by the front of the debris cloud.

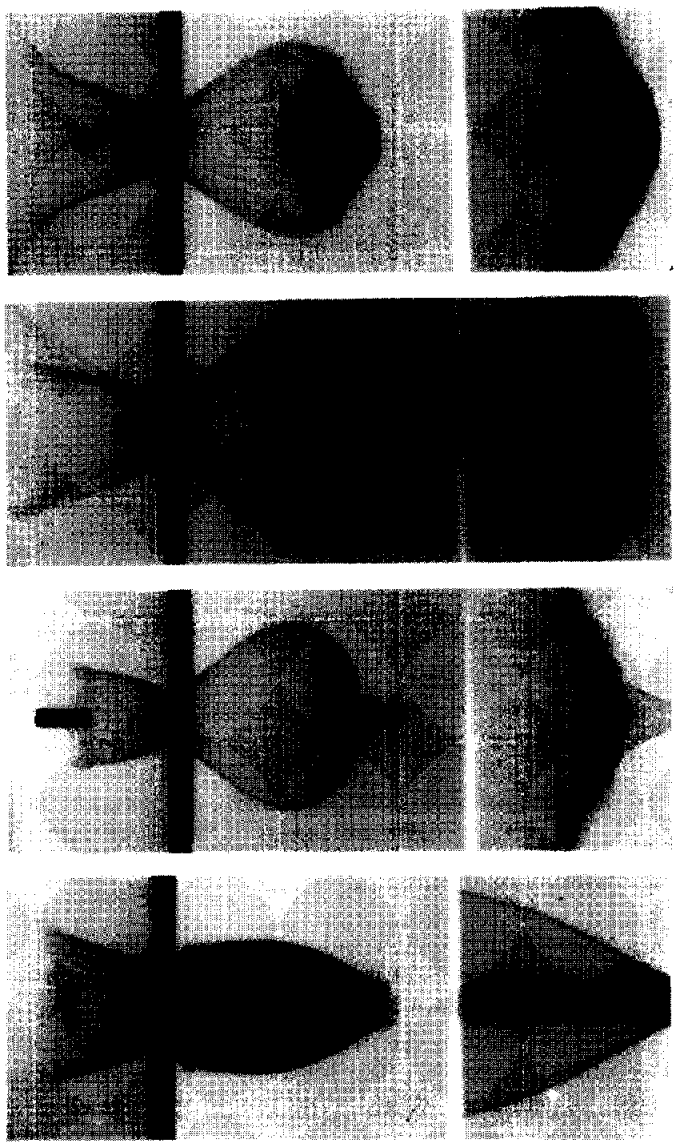

Fig. 2. Radiographs of debris clouds produced by the impact of four different shapes of zinc projectiles with 0.965-mm-thick zinc sheets.

The debris cloud formed by the disk contained a long columnar structure inside the external bubble of debris. Several small features of the columnar structure elongated as the debris cloud moved downrange, indicating that the structure was composed of very small fragments and/or droplets. This internal columnar structure was considered to be a "porous rod" composed of bumper and projectile material. The impact of the columnar structure with the rear wall produced a 1.4-cm-diameter hole in the wall. Increasing or decreasing the spacing between the bumper and rear wall would have had little effect on the damage to the wall, since the column did not display any tendency to disperse as it moved downrange.

The effect of the inclination of the axis of a cylindrical projectile on the details of the debris cloud produced by the impact of an inclined cylinder are shown in the orthogonal-pair of radiographs presented in Fig. 3. The projectile shown in the radiographs is a three-quarter hard, OFHC copper disk with an *L/D* of 0.3. The bumper was a 2.03-mm-thick, 6061-T6 aluminum sheet. In this test, copper and aluminum were used as the projectile and target, respectively, to

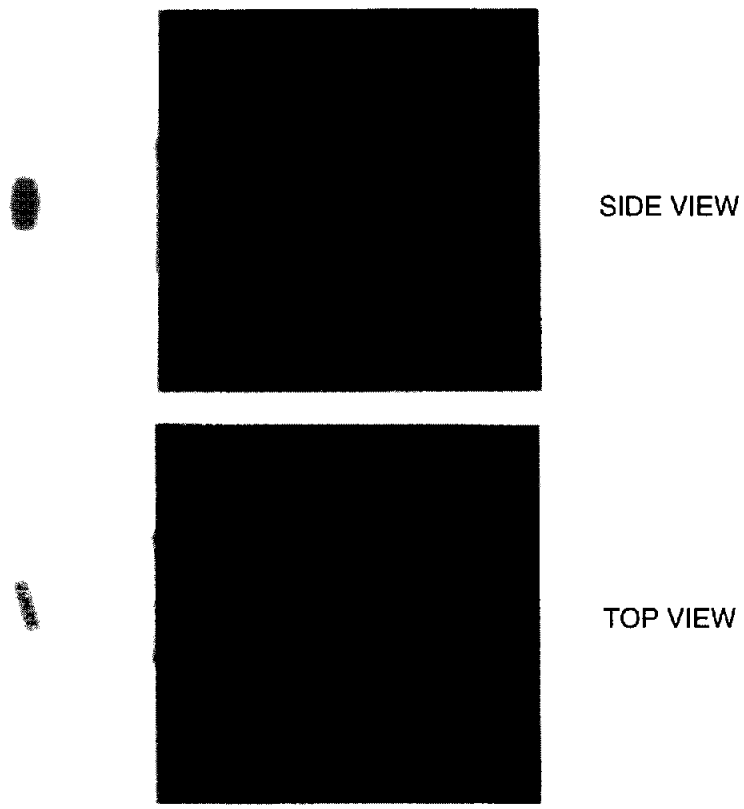

Fig. 3. Orthogonal-pair of radiographs of the debris cloud produced by the impact of an inclined copper disk with an aluminum sheet at 6.47 km/s.

facilitate the determination of the source of material in the various elements of the debris cloud. The difference in the x-ray absorption characteristics of the two materials makes them easy to identify in the radiographs. The debris cloud shown in Fig. 3 also exhibits the three major features identified in the debris clouds produced by the impact of spheres—an ejecta veil, an external bubble of debris, and an internal structure. The fragmented copper disk is totally contained within an external bubble of aluminum debris. The cone-shaped structure at the leading edge of the external bubble of debris is composed of fragments of bumper material. The large dark, cone-shaped structure inside the external bubble of debris is projectile material. The axes of both of the cone-shaped structures are inclined in the same direction as the axis of the disk at impact. The magnitude of the angle of these features is a function of the inclination of the projectile axis and the distance from the bumper to the feature.

An examination of the top-view radiograph in Fig. 3 shows that the upper portion of the inclined surface of the front cone and the lower portion of the inclined surface of the rear cone form surfaces that are tending to be parallel to the shot-line axis. When the axis of the projectile is inclined appropriately, one or both of these surfaces will be roughly parallel to the shot-line axis. Since the bulk of the projectile fragments were shown in [7] to be located at the periphery of the conical structures, the impact of the fragments in these critically aligned surfaces is capable of forming large holes in the rear wall of a simple Whipple shield. The effect of a change in the inclination angle of the projectile is related, in Figs. 4 and 5, to the damage patterns produced on the rear walls of double-sheet structures impacted by right-cylinders of aluminum. The spacing between the rear surface of the bumper and the front surface of the rear wall was maintained at 10.59 cm for the tests presented in Fig. 4. Inclination of the cylinder at impact and

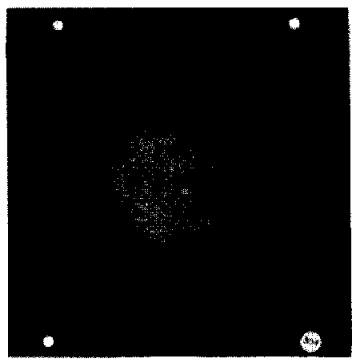

7 DEGREE INCLINATION, 6.48 km/s

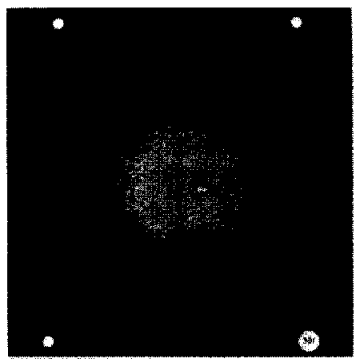

12 DEGREE INCLINATION, 6.30 km/s

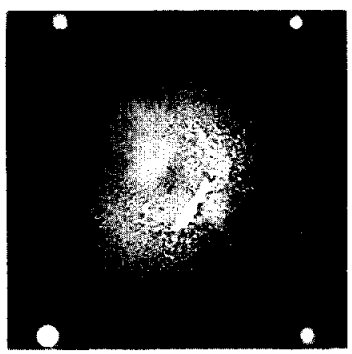

18 DEGREE INCLINATION, 6.31 km/s

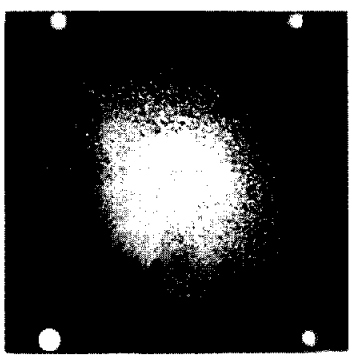

25 DEGREE INCLINATION, 6.39 km/s

Fig. 4. Damage patterns produced on 6.35-mm-thick, aluminum rear walls by debris clouds formed by the impact of inclined, 1 g aluminum right cylinders with 2.03-mm-thick aluminum sheets.

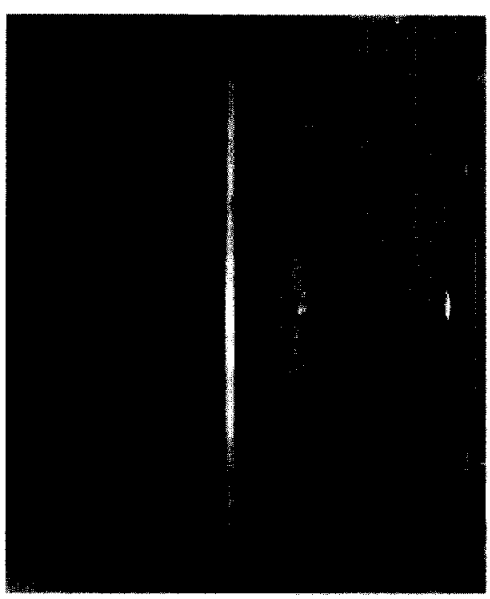

Fig. 5. Damage pattern formed on a 5.72-mm-thick, aluminum rear wall by the debris cloud formed by the impact of an inclined (~45 degrees), 1 g aluminum right cylinder with a 2.03-mm-thick aluminum sheet at 6.24 km/s. Bumper and rear wall are 10 cm apart.

features of the debris clouds were determined using an orthogonal pair of flash x-rays to view the projectile and two orthogonal pairs of x-rays to view the debris cloud.

Large spall failures were formed on the rear surface of all of the rear walls shown in Fig. 4. The rear walls for the tests with 7 and 12 degrees of inclination were not perforated although a deep crater was formed near the center of the rear wall for the 7-degree test. In addition, there is a variation in the density of the smaller craters in the region surrounding the central crater. A shallow central crater is evident in the rear wall for the 12-degree test. The concentration of craters in the region to the left of the shallow central crater is considerably heavier than it is to the right of the central crater. In the 18-degree test, the "central" crater is smaller and a significant distance from the center of the rear wall. A well defined, heavily cratered, crescent-shaped region is shown to the left of the "central" crater while the region to the right of the "central" crater shows little evidence of impact. A through crack has developed along most of the length of the heavily cratered, crescent-shaped region. A small "central" crater is not evident on the rear wall for the 25-degree test. As shown in this test, a further increase in the inclination angle of the projectile has resulted in a more dramatic separation of the regions noted in the description of the damage patterns for the other three tests. The concentration of craters in the crescent-shaped region has intensified and is dominated by a large hole. The extent of the region that shows little evidence of impact has also increased significantly.

The aluminum right cylinder that impacted the double-sheet target and multiple witness plates shown in Fig. 5 was inclined approximately 45 degrees before impact. Pre-impact inclination of the projectile was determined from films taken with a synchroballistic streak camera while the cylinder was in flight. Although the rear-wall damage pattern in Fig. 5 is similar to the pattern shown for the 25-degree test in Fig. 4, the extent of the heavily cratered and the lightly cratered regions is more pronounced in Fig. 5.

A comparison [2] of the structural features observed in the radiographs of the debris clouds that produced the rear-wall damage patterns shown in Fig. 4 identifies the source of the fragments producing the damage. The material forming the tip of the front cone of bumper fragments produced the "central" crater. The radiographically dense regions of the inner cone of projectile fragments produced the heavily cratered, crescent-shaped regions where cracking and/or perforation of the rear wall occurred. Although radiographs were not available from the test shown in Fig. 5, the features of the rear-wall damage pattern are consistent with the trend in damage patterns observed in the rear walls shown in Fig. 4.

IRREGULAR-SHAPED PROJECTILES

The debris clouds shown thus far were produced by the impact of projectiles with regular shapes. The shape and orientation of the projectile at impact were shown to affect the characteristics and properties of the debris clouds. On occasion, spheres used in tests are struck by debris from the sabot-stripper plate and are chipped or deformed prior to impact with a bumper sheet. Radiographs of debris clouds produced by the 7.2 km/s impacts of 6.35-mm-diameter, 2017-T4 aluminum spheres with nominally 0.32-mm-thick, 6061-T6 aluminum bumper sheets are shown in Fig. 6. A typical debris cloud formed by the impact of a "clean" sphere is shown in the upper radiograph. The sphere in the center radiograph was heavily damaged by stripper-plate debris before it struck the bumper. A section of the upper rear of this sphere was removed and the portion that remained may have been broken into several large pieces. The debris cloud formed by the damaged sphere was considerably different than the debris cloud produced by the "clean" impact. The debris cloud formed by the damaged sphere was a cluster of randomly-spaced fragments of projectile and bumper debris, in contrast to the well-developed, symmetric structure formed by the impact of the intact sphere. As shown in the late-time view of the debris cloud in the lower radiograph, many of the damaged-sphere fragments were quite large when compared to the fragments produced by the impact of the undamaged

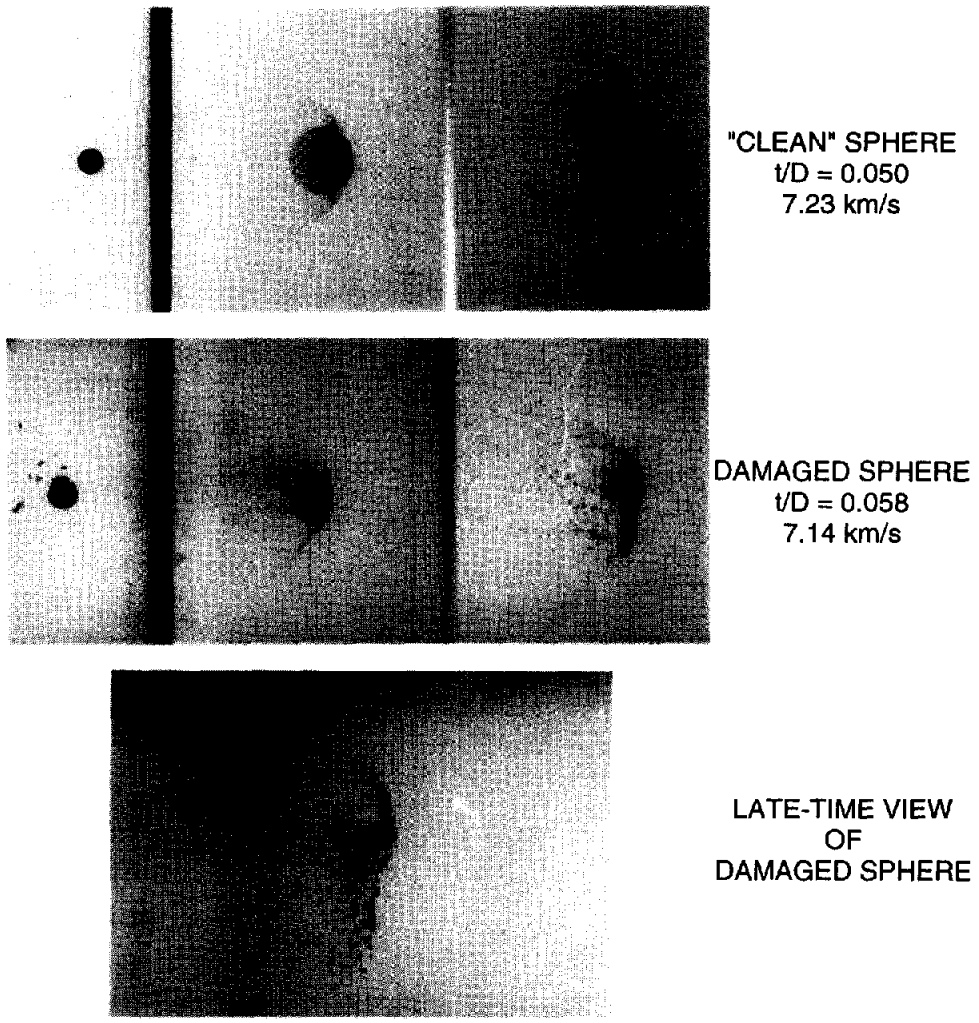

Fig. 6. Radiographs of debris clouds produced by the impact of 6.36-mm-diameter, 2017-T4 aluminum spheres with 0.32-mm-thick, 6061-T6 aluminum sheets.

sphere. The debris cloud formed by the damaged sphere may be more typical of a debris cloud produced by the impact of a large micrometeoroid or chunky fragment of orbital debris.

The damage pattern formed on a rear wall by the debris cloud produced by the impact of a "clean" 9.53-mm-diameter, aluminum sphere with a 2.22-mm-thick aluminum sheet is shown at the top of Fig. 7. The damage pattern formed by the debris cloud produced by the impact of a damaged 9.53-mm-diameter, aluminum sphere with a 2.22-mm-thick aluminum sheet is shown at the bottom of Fig. 7. The rear of the damaged sphere was struck by a very small steel chip from the sabot stripper but was not heavily damaged. Because of a pre-trigger produced by the "dirty" environment surrounding the damaged sphere, the timing sequence for the firing of the x-ray sources was altered. As a result, the first and only view of the debris cloud was of its leading edge and was taken about 22 μs after impact. Features of the leading edge of the cloud appeared to be identical to the features of the leading edge of the debris cloud for the "clean" sphere. The inner rings of the damage patterns were similar in shape and size for both tests. The outer ring for the damaged sphere was distorted, however. The damage to the rear of the sphere resulted in the formation of an asymmetric spall shell and a distorted outer ring in the damage pattern. It was not clear whether the three small holes in the rear wall in the area of the disturbance in the

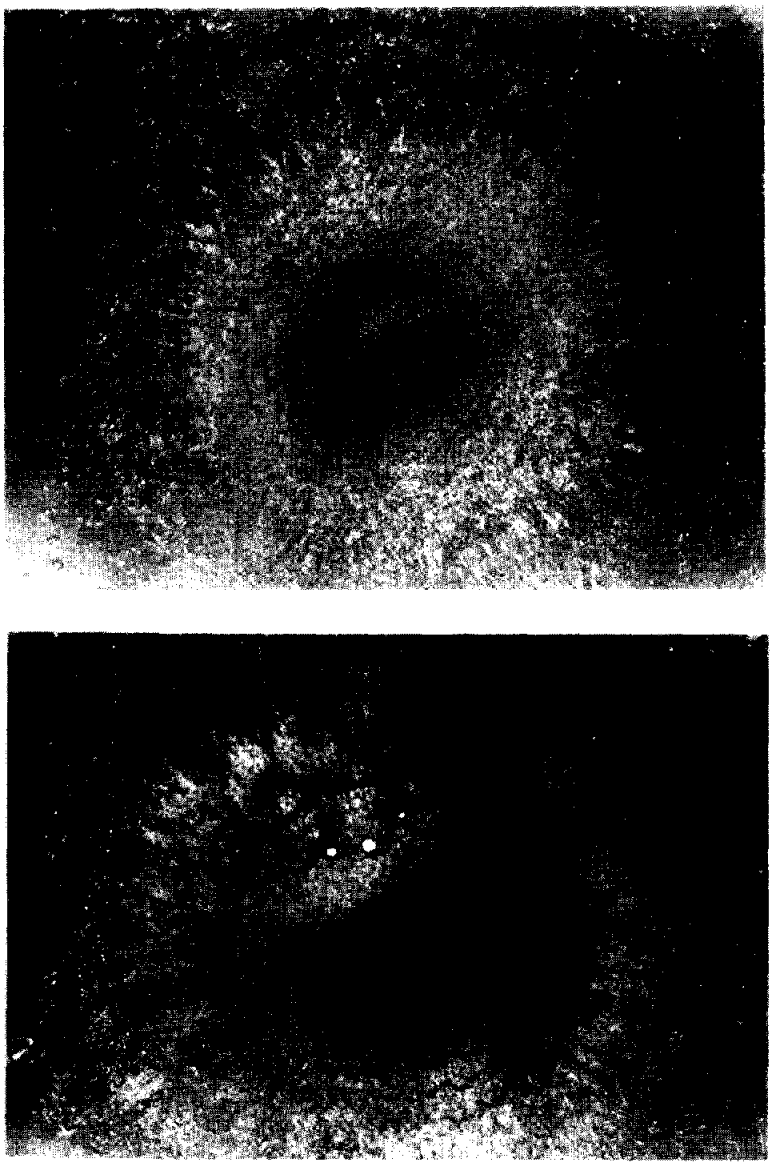

Fig. 7. Damage patterns produced by debris clouds formed by the impact of a "clean" and a damaged 9.53-mm-diameter, 2017-T4 aluminum sphere with 2.22-mm-thick, 6061-T6 aluminum sheets.

outer ring were caused by the impact of fragments from the rear of the sphere or by the impact of steel chips from the stripper. It is remarkable that a small irregularity in the rear surface of the sphere was capable of affecting the damage pattern formed by the debris cloud produced by the damaged sphere.

An orthogonal pair of radiographs showing the debris cloud produced by the impact of a 7075-T6 aluminum sabot insert with a 0.965-mm-thick zinc bumper sheet are presented in Fig. 8. The insert was one of a pair that was placed inside the nylon sabot used during the launch of the L/D = 3 zinc rods shown in Fig. 2. The sabot apparently failed at some point during the launch process or was damaged during the sabot-stripping operation. The insert separated from the sabot and traveled to the target. The radiographs showed that it impacted the bumper sheet with its base end forward and was eroded to the hole seen in the pre-impact view of the insert. The

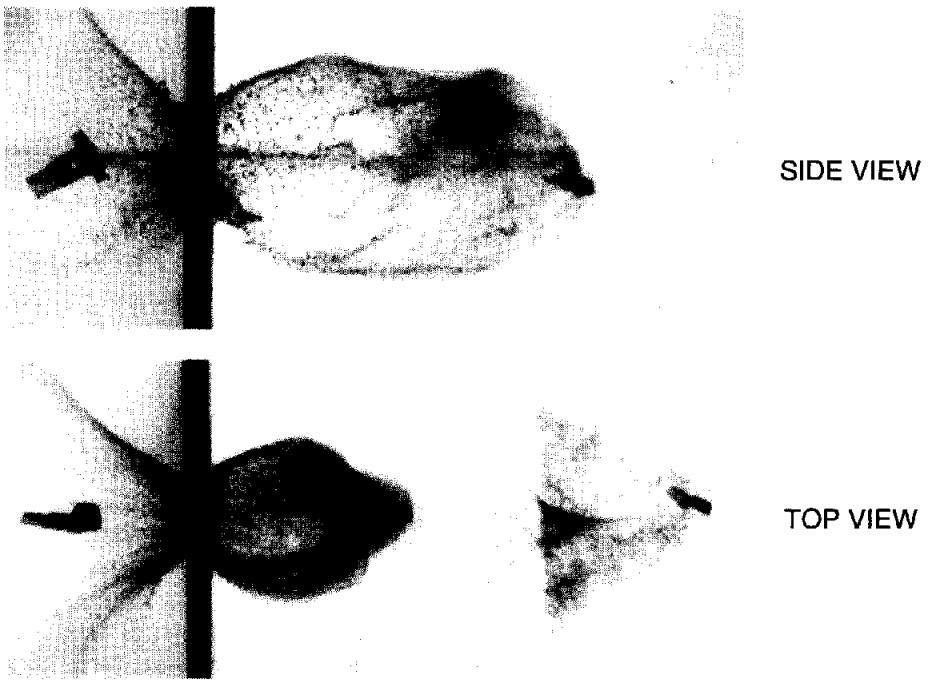

Fig. 8. Radiographs of the debris cloud produced by the impact of a 7075-T6 aluminum sabot insert with a 0.095-mm-thick zinc sheet.

front of the debris cloud is asymmetric, with the eroded sabot insert just inside the leading edge of the cloud.

The radiographs of the debris clouds produced by the normal impact of irregularly shaped projectiles (i.e., the damaged sphere in Fig. 6, and the sabot insert in Fig. 8) show one or more large, irregularly-shaped pieces of the projectile intact and at the *leading edge* of the debris cloud. By contrast, the large central fragment produced by the normal impact of a sphere with a thin sheet was always a short distance *behind* the front element of the debris cloud. The size and location of these large, irregularly-shaped pieces of projectile in the debris cloud, makes these fragments a serious threat to the rear wall of a double-sheet structure.

DISCUSSION

Examination of the radiographs of debris clouds produced by the impact of nonspherical projectiles showed that the projectile fragments in the debris cloud were always large and/or a portion of the projectile was left intact and that these large projectile fragments were at the front of the debris cloud. Because of their size and position in the debris cloud, these large fragments are a severe threat to the integrity of the rear wall of a spacecraft. Tests employing identical targets, spherical projectiles with the same mass, and fired at normal incidence with the same impact velocities would indicate that the rear wall of the structure would resist penetration.

The cause of the reduced effectiveness of bumper shields in promoting the disintegration of nonspherical projectiles and spheres impacting at obliquity must be related to the nonuniform propagation of impact-induced shocks and stresses in the bumper and projectile. Propagation of the impact-induced shock in a sphere is an axisymmetric process. When a sphere impacts a thin sheet at hypervelocity, shocks form and propagate into the sphere and the sheet. The intensity of the shock and the extent of its influence on the sphere and the sheet are a function of the t/D ratio and the impact velocity of the sphere. When a disk or short cylinder (length-to-diameter ratio of

one or less) impacts a thin sheet at normal incidence, with the axis of the disk coincident with the shot-line axis, a one-dimensional shock propagates in the projectile and the bumper. During the impact of inclined cylindrical projectiles and nonspherical projectiles with thin bumper sheets, the propagation of the shocks in the projectile and the bumper are not symmetric or predictable processes. The orientation of local features of the projectile may or may not promote shock loading in the region of the feature. In many instances, a shock generated in the bumper or projectile will outrun the point of contact between their impacting surfaces. As a result, subsequent contact between the surfaces will involve interactions of previously disturbed material. Loads generated by impacts with postshocked material may be considerably lower than loads generated by impacts with unshocked material because of microscopic changes in the structure of the previously shocked material. Reduced impact loading of the projectile would result in the formation of larger fragments in the debris clouds.

SUMMARY

Evaluations of the effectiveness of spacecraft shields that are based on the results of tests that used "relatively benign" spheres as simulants of an unknown threat (unknown in mass, shape, density, impact velocity, and angle of incidence) must be tempered with the realization that the real threat is likely to more severely challenge the shield structure.

The aspect ratio, *L/D*, of cylindrical projectiles can have a pronounced effect on the ability of the debris cloud produced by the impact of the cylindrical projectile to cause failure of a shield. In general, for a given impact velocity, the mass of a cylindrical projectile required to defeat a shield will be less than the mass of a sphere required to defeat the same shield. Debris clouds produced by disks impacting with their axis coincident with their line of flight were shown to be particularly effective penetrators since the fragmented projectile merely formed a "column" of particles that did not disperse laterally as it moved downrange. The inclination of certain regular-shaped projectiles at impact was also shown to affect the lethality of the debris cloud. Debris clouds produced by inclined projectiles were considerably more damaging.

Acknowledgement—A portion of this work was supported by the Office of the Director of the University of Dayton Research Institute and by NASA Marshall Space Flight Center under Prime Contract NAS 8-38856 on Subcontract A71447 with Lockheed Martin. The author wishes to acknowledge Dr. Joel Williamsen formerly of NASA-MSFC (now at Denver Research Institute) and Dr. Norman Elfer of Lockheed-Martin for their support of the original work and Dr. Lalit Chhabildas of Sandia National Laboratory for the use of the radiographs from the tests with zinc projectiles and bumpers.

REFERENCES

[1] Morrison RH. Investigation of projectile shape effects in hypervelocity impact of a double-sheet structure. NASA TN D-6944, August 1972.

[2] Piekutowski AJ. Debris clouds generated by hypervelocity impact of cylindrical projectiles with thin aluminum plates. *Int. J. Impact Engng.* 1987; **5**: 509-518.

[3] Piekutowski AJ. Properties of largest fragment produced by hypervelocity impact of aluminum spheres with thin aluminum sheets. *Proc. AIAA Space Programs and Technologies Conference,* Huntsville, AL, 1992: Paper No. 92-1588.

[4] Piekutowski AJ. Formation and description of debris clouds produced by hypervelocity impact. NASA CR-4707, February 1996.

[5] Piekutowski AJ. Effect of scale on debris cloud properties *Int. J. Impact Engng.* 1997; **20**: 639-650.

[6] Konrad CH, Chhabildas LC, Boslough MD, Piekutowski AJ, Poormon KL, Mullin SA, Littlefield DL. Dependence of debris cloud formation on projectile shape. In: Schmidt SC, Shaner JW, Samura GA, Ross M., editors, *High-Pressure Science and Technology–1993*, AIP Press, New York, NY, 1994. American Institute of Physics AIP Conference Proceedings 309, Part 2, p.1845-1848.

[7] Piekutowski AJ. A simple dynamic model for the formation of debris clouds. *Int. J. Impact Engng.* 1990; **10**: 453-471.